Cryotherapy with concurrent CpG oligonucleotide treatment controls local tumor recurrence and modulates Her2/neu immunity

Jesse J. Veenstra[1], **Heather M. Gibson**[2], **Peter J. Littrup**[2], **Joyce D. Reyes**[2], **Michael L. Cher**[2,3], **Akira Takashima**[4], and **Wei-Zen Wei**[1,2]

[1]Department of Oncology, Wayne State University School of Medicine, Detroit, MI 48201

[2]Karmanos Cancer Institute, Detroit, MI 48201

[3]Department of Urologic Oncology, Wayne State University School of Medicine, Detroit, MI 48201

[4]Department of Medical Microbiology and Immunology, University of Toledo College of Medicine, Toledo, OH, 43606

Abstract

Percutaneous cryoablation is a minimally invasive procedure for tumor destruction, which can potentially initiate or amplify antitumor immunity through the release of tumor-associated antigens. However, clinically efficacious immunity is lacking and regional recurrences are a limiting factor relative to surgical excision. To understand the mechanism of immune activation by cryoablation, comprehensive analyses of innate immunity and Her2/neu humoral and cellular immunity following cryoablation with or without peritumoral CpG injection was conducted using two Her2/neu$^+$ tumor systems in wild type, neu-tolerant, and SCID mice. Cryoablation of neu$^+$ TUBO tumor in BALB/c mice resulted in systemic immune priming, but not in neu-tolerant BALB NeuT mice. Cryoablation of human Her2$^+$ D2F2/E2 tumor enabled the functionality of tumor-induced immunity but secondary tumors were refractory to anti-tumor immunity if rechallenge occurred during the resolution phase of the cryoablated tumor. A step-wise increase in local recurrence was observed in wild type, neu-tolerant, and SCID mice indicating a role of adaptive immunity in controlling residual tumor foci. Importantly, local recurrences were eliminated or greatly reduced in wild type, neu tolerant and SCID mice when CpG was incorporated in the cryoablation regimen, showing significant local control by innate immunity. For long-term protection, however, adaptive immunity was required because most SCID mice eventually succumbed to local tumor recurrence even with combined cryoablation and CpG treatment. This improved understanding of the mechanisms by which cryoablation affects innate

The authors disclose no potential conflicts of interest.

and adaptive immunity will help guide appropriate combination of therapeutic interventions to improve treatment outcomes.

Keywords

Cryotherapy; CpG; Her2/neu; immunomodulation

Introduction

As immunotherapy becomes a mainstay in cancer therapy, attention is directed to immune constituents in the tumor microenvironment, particularly the modulation of their activities to enhance treatment outcomes. In parallel with this progress is the advancement in image guided percutaneous cryoablation that utilizes ultra-cold temperatures to precisely destroy cancers of the breast, prostate, kidney, liver, bone, lung, brain, and skin (1). Cryoablation directly induces necrosis by damaging cell membranes and organelles via the formation of ice crystals, and indirectly through osmotic stress and ischemia from thrombosis of the microvasculature (2). Compared to surgical resection, cryoablation is minimally invasive, places less stress on the body, allows for quicker recovery, and is less costly (3). In addition to debulking the tumor, the necrotic tissue becomes a rich reservoir of tumor-associated antigens that are cleared by antigen presenting cells (APCs), creating a unique opportunity to prime or boost systemic antitumor immune responses, which may afford increased survival (4).

Induction of systemic immunity was initially observed in the 1970's when several patients had metastatic lesions regress following cryoablation of primary prostate tumors (5). Further support of 'cryoimmunology' was linked to an increase in antibodies against DNA, RNA, and tumor cells in patients receiving palliative cryoablation for advanced cancer (6). More recently a study following 20 prostate cancer patients observed elevated levels of circulating inflammatory cytokines and cellular immunity after cryotherapy but found responses were transient and unable to prevent disease relapse (7). In a separate study, cryoablation of metastatic renal cell carcinoma resulted in elevated T-cell and antibody (Ab) responses without affecting the growth of untreated foci (8). While these results stimulated interest in the immunostimulatory potential of cryoablation, mechanisms leading to beneficial immunity have yet to be elucidated.

Although enhanced immune priming after cryoablation has been described in a number of pre-clinical studies (9-11), others indicate that cryoablation does not elicit any change in tumor-specific immunity (12-14), or worse, induces immune suppression and tumor progression (15-17). The inconsistencies in tumor-specific immunity and rejection of distant tumors reflect an inadequate understanding of the mechanisms of immune priming and suppression associated with cryoablation. The discrepancy in findings is, at least in part, due to the wide range of tumor models assessed and their varying immunogenicity in respective hosts.

To begin elucidating and exploiting the immunological mechanisms of cryotherapy, we evaluated antitumor immunity following cryoablation of BALB/c mouse mammary

adenocarcinomas TUBO and D2F2/E2, which respectively express rat neu and human Her2 and exhibit well-characterized immunogenicity in wild type (WT) and neu-tolerant transgenic mice. To further amplify and modulate cryoablation induced immunity, we also tested a Toll-like receptor (TLR) 9 agonist, CpG oligodeoxynucleotides. Dendritic cells (DC) and B-cells are the primary cell types that express TLR9, although mice have additional expression on monocytes and macrophages (18). Activation of these cells by CpG initiates stimulatory pathways that results in the indirect maturation, differentiation, and expansion of additional DCs, T-cells, NK cells, and macrophages (19-21). These cells subsequently secrete cytokines that generate a pro-inflammatory and strongly Th1 biased environment (21-23). These conditions enhance cytotoxic T-cell responses and inhibit Th2-mediated suppression, which is associated with more efficacious antitumor immunity (24). Previous work by den Brok *et al* initially found that peritumoral injection of CpG immediately following tumor cryoablation results in more robust systemic tumor protection via increased DC maturation and cross-presentation of the model tumor antigen OVA (25, 26). The study focused on DC activation but did not assess antigen specific Ab responses or other innate immune activation after treatment. In this study we provide a comprehensive evaluation of innate immunity and α-Her2/neu adaptive immunity following cryoablation with or without CpG as well as tumor excision using two tumor systems in WT, immune-tolerant, and SCID mice. Importantly, we assessed the impact of peritumoral CpG injection on local recurrence, which is a potential clinical limitation for cryoablation of locally aggressive or high-risk tumors (27, 28).

Materials and Methods

Mice

Female BALB/c and SCID/NCR (BALB/c background) mice (6-8 week old) were purchased from Charles River Laboratory. Heterozygous C57BL/6 pIL-1β-DsRed transgenic mice have previously been described (29). Heterozygous IL-1β-DsRed (BALB/c x C57BL/6) F1 mice were generated by crossing heterozygous C57BL/6 DsRed males with wild type (WT) BALB/c mice and screened for transgene expression. Heterozygous BALB/NeuT female mice, which express a transforming rat *neu*, develop atypical ductal hyperplasia at 3 weeks of age which progresses to carcinoma *in situ* and then palpable tumors between 16 and 18 weeks of age (30, 31). All animal procedures were approved by and performed in accordance with the regulation of Wayne State University Animal Investigation Committee.

Cell lines

The neu+ TUBO line cloned from a spontaneous mammary tumor in a female BALB NeuT mouse was obtained through Dr. Guido Forni (U. Torino, Torino, Italy) (32). The D2F2 line was established in our group from a spontaneous mammary tumor that arose from the prolactin-induced hyperplastic alveolar nodule line, D2 (33). The mouse origin of TUBO and D2F2 was verified by spectral karyotyping (34) and aliquots of frozen stock were thawed for short term culture in each experiment. Each individual culture was verified by flow cytometry using mAb M1/42 to BALB/c MHC I. BALB/c mice inoculated with TUBO or D2F2 cells develop progressive tumors to validate their BALB/c origin. D2F2 cells

transfected with human Her2 (35) were passaged through BALB/c mice to select D2F2/E2 that maintains Her2 expression in vivo. Antigen presenting cells (APC) 3T3/EKB and 3T3/NKB were generated by transfecting NIH3T3 cells (American Type Culture Collection) with Kd, B7.1 (CD80), and Her-2 (EKB) or neu (NKB) as we described (36). Expression of these molecules are monitored monthly by flow cytometry.

Tumor Inoculation and DNA vaccination

Mice were inoculated with 2.5×10^5 tumor cells in mammary fat pad #4 (left) or #9 (right). Tumor growth was monitored by palpation and caliper measurement. Tumor volume was calculated as $v = (l \times w^2) / 2$. Recurrent tumors were defined as new growth at the primary site after treatment completion.

For DNA vaccination, an admix of 30 μg each of pGM-CSF and pNeu-E2$_{TM}$ encoding a rat neu and human Her2 fusion protein or pVax1 (control) in 50 μL PBS was injected i.m. in the left gastrocnemius followed immediately by application of electrode gel and square wave electroporation using a BTX830 (BTX Harvard Apparatus) (35).

Cryoablation and surgical procedures

Cryoablation was performed on tumors ~4x7 mm (~60 mm^3) in size, using the argon-based CryoCare system with the 1.7mm diameter PERC-15 Percryo CryoProbe – round ice (Endocare). Briefly, an ellipse of skin over the tumor was removed, and the tumor was retracted without interrupting tumor vasculature. The cryoprobe was longitudinally inserted through the tumor and freezing was initiated at 100% power for 1 minute reaching -150°C, followed by the thawing cycle, which lasted ~1 minute. After two freeze-thaw cycles were completed, the skin was closed over the tumor. Sham surgery was identically performed without freezing and thawing. Surgical excision was performed using electrocautery to remove the tumor and adjacent mammary tissue. Incisions were closed using surgical staples.

CpG ODN mu2395

The murine specific class C CpG sequence: 5'-TCGACGTTTTCGGCGCGCGCCG-3' with a phosphorothioated backbone (Integrated DNA Technologies) was designed by substituting the human hexamer motif (5'- GTCGTT-3') for the optimal mouse motif (5'-GACGTT-3') in the C-Class ODN 2395 (37). One hundred μg of CpG was administered peritumorally over 3 injection sites: lateral, caudal, and rostral mammary tissue relative to tumor (10 μL/ injection site).

Imaging and histology of cryoablated tumors

Tumors were removed from WT or IL-1β-DsRed BALB/c x C57BL/6 F1 mice and imaged immediately in the In-Vivo MS FX PRO (Carestream) in the Microscopy, Imaging, and Cytometry Resources (MICR) core. Fluorescent spectra collected for 30 seconds were merged with white light images. Mean DsRed fluorescence of each tumor slice was quantified using ImageJ densitometry software. Hematoxylin and eosin (H&E) staining was performed in the Animal Model and Therapeutics Evaluation Core. Histology images were captured using the SCN400 slide scanner and software (Leica Microsystems).

Antibody measurement

Her2 and neu specific IgG levels in the serum were quantified by flow cytometry with a BD FACSCanto II (Becton Dickinson) (MICR core), using Her2 expressing SKOV3 cells or neu transfected 3T3/NKB cells as previously described (38). Normal mouse serum was a negative control. An Ab5 (α-Her-2 mAb TA-1, Calbiochem) or Ab4 (α-neu mAb, 7.16.4, Calbiochem) equivalent for Her2 and neu binding Ab, respectively, was calculated by regression analysis. Area under the curve (AUC) for Ab levels was measured for each mouse using the equation ((Day Y) – (Day X)) x (Ab X + Ab Y) / 2 between two time points where Day Y follows Day X. The sum of values for all time points makes up the AUC.

In vitro antigen stimulation and multiplexing

Lymph node cells (LNs) or splenocytes were enumerated using the Cellometer Vision (Nexcelom) and added to a 24 well plate (8×10^5 cells/well). 3T3/EKB or 3T3/KB were treated with 10 μg/mL Mitomycin C for 3 hours before co-incubation with LNs or splenocytes (8×10^4 cells/well). Supernatants were collected after 48 hours.

The levels of GM-CSF, IFN-γ, IL-1β, IL-2, IL-4, IL-5, IL-6, IL-10, IL-12 (p40/p70), and TNF-α were quantified in cell culture supernatant or plasma samples using the Cytokine Mouse Magnetic 10-Plex kit (Life Technologies) with the Magpix platform (Luminex) according to the manufacturer's instructions.

IFN-γ ELISPOT

Antigen specific IFN-γ production was measured by ELISPOT assay as previously described (38). Engineered APCs were incubated with LNs or splenocytes for 48 hrs. Spots were enumerated with the ImmunoSpot analyzer (CTL). Results were expressed as spot forming units (SFU) per 10^6 cells.

Cell phenotyping

Peripheral blood mononuclear cell (PBMC) phenotyping was performed with flow cytometry using a BD FACSCanto II (Becton Dickinson) (MICR core). Approximately 2×10^6 PBMC were incubated for 15 min on ice in flow buffer (0.25% FBS in 1x PBS) with anti-mouse CD16/CD32 (2.4G2) (BD Pharmingen). Cells were stained with the eFluor 780 viability dye (eBioscience) and the following: α-TCRβ (H57-597), α-CD11c (N418), α-CD49b (DX5). All antibodies were from eBioscience. Data were analyzed using FlowJo software (Tree Star). All populations enumerated as percentage of viable singlets.

Statistical analyses

Statistical analyses were conducted using GraphPad Prism 6. Error bars shown represent SEM unless otherwise noted. Survival percentages were calculated using the Kaplan-Meier method and significance determined by log-rank test (39). For Kaplan-Meier curves, symbols indicate censored subjects due to experimental endpoint. All tests use one-way ANOVA with Tukey's post-test unless otherwise noted. *P* values less than 0.05, 0.01, and 0.001 are noted as *, **, and ***, respectively.

Results

Necrosis and inflammatory infiltration following tumor cryoablation

To evaluate cellular responses to cryoablation, BALB/c mice inoculated with neu[+] TUBO adenocarcinoma were treated with cryoablation and tumors were removed 1, 3, 9, and 29 days later for H&E histology (Fig. 1). Complete coagulative necrosis in the ablated tissue was evident by the absence of nuclear staining. Consistent with the classical wound healing process, polymorphonucleocytes (PMNs) in the peripheral and perivascular regions of the tumor were apparent 1 day after cryoablation (Fig. 1A) and dissipated by day 3 (40). Macrophage and fibroblast infiltration was evident by day 9 (Fig. 1A). Over the next 4 weeks, fibroblasts continued to expand and produce collagen, indicative of tissue remodeling.

To detect functional inflammatory infiltrates in cryoablated tumors, D2F2/E2 mammary tumor was inoculated into pIL-1β-DsRed transgenic (BALB/cxC57Bl/6 F1) mice, which utilize IL-1β promoter to drive the fluorescent marker gene DsRed. Mice received cryoablation or sham surgery when tumors reached ~60mm^3. On day 15 post-treatment, tissues were removed for *ex vivo* imaging on a Carestream MS FX Pro *in vivo* imager (Fig. 1B). Mean densitometry of tumor slices showed significantly greater DsRed fluorescence in cryoablated tumors relative to sham treated tumors (Fig. 1C). This finding provides direct evidence of IL-1β activation, consistent with inflammatory infiltrates in ablated tissues.

Cryoablation of TUBO mammary adenocarcinoma induces α-neu IgG and systemic tumor protection

To test if cryoablation induces systemic tumor immunity, BALB/c mice were inoculated with neu^{+} TUBO cells. When tumors reached ~60mm^3 they were treated with cryoablation with or without CpG injection, CpG alone, surgical excision, or left untreated (n=6-8) (Fig. 2A). All tumors treated with cryoablation ± CpG or surgical excision completely regressed except two mice in the cryoablation group that developed recurrences on day 41 and 57. CpG treatment alone did not cause regression but reduced tumor growth relative to untreated mice (Fig. 2B).

Once cryoablated tumors had fully resolved (~8 wks), tumor-free mice received a secondary TUBO inoculation on the contralateral side to simulate outgrowth of a distant tumor. Cryoablation of the primary tumor protected 6/11 (55%) mice from secondary inoculation, whereas addition of CpG to cryoablation protected 15/16 (94%) mice (Fig. 2C-D). Thus, cryoablation of TUBO induced systemic antitumor immunity that was significantly enhanced by concurrent TLR9 stimulation via CpG. In contrast, surgical excision eliminated the primary tumor without triggering immune priming and only 1/6 mice rejected the secondary inoculation. These results suggest cryoablation, but not surgical excision released tumor associated antigens to prime tumor specific adaptive immunity.

In a fraction of cryoablation treated mice it was noted that primary tumors recurred but not if CpG was concurrently used. To further investigate this finding, recurrences were compiled from 4 independent experiments to include mice treated with either cryoablation alone or cryoablation + CpG. All mice were treated when tumors were ~60mm^3 and monitored for

30-90 days (Fig. 2E). Cryoablation alone had a recurrence rate of ~26%, occurring between 34-60 days. When CpG was combined with cryoablation the recurrence rate fell to 0%. Surgical excision of similar size tumors, produced no detectable recurrences (n=24) (not shown). Therefore, equivalent long-term recurrence rates as surgical resection can be achieved with cryoablation if CpG is used concurrently in WT mice.

To determine the mechanism of tumor rejection by cryoablation α-neu humoral and cellular immune responses were measured. Several reports have shown α-neu Ab is sufficient for rejection of TUBO tumor (32, 36, 41). We found inoculation and growth of TUBO in naïve mice did not induce α-neu IgG (Supplementary Fig. S1 A), suggesting a block or lack of antigen presentation by the untreated tumor. Using DNA electrovaccination as previously described (35), a hybrid rat neu / human Her2 DNA construct (pNeuE2) induced α-neu IgG to correlate with TUBO regression (Supplementary Fig. S1 B), suggesting tumor regression by α-neu Ab. Thus, TUBO may resemble Herceptin sensitive breast cancer the immune system can potentially recognize but does not without exogenous manipulation (42).

Mice treated with cryoablation produced α-neu IgG beginning 14 days postoperatively (16±7 μg/mL) and plateaued thereafter (Fig. 3A). Injection of CpG without cryoablation also induced α-neu IgG (22±7 μg/mL), although tumors failed to regress (Fig. 2B). When CpG was used in combination with cryoablation, α-neu IgG levels increased to 58±16 μg/mL at day 41, and remained elevated to at least day 70, indicating immune synergy between cryoablation and CpG injection. Area under the curve (AUC) analysis found significant differences occurring between cryoablation + CpG and cryoablation groups, as well as between cryoablation and excision groups. Mice undergoing surgical excision produced very low levels of α-neu IgG (1.5±0.03 μg/mL) similar to untreated tumor-bearing mice (Fig. 3A). Additionally, cryoablation + CpG induced both IgG1 and IgG2a, whereas cryoablation alone induced primarily IgG1 (Fig. 3B). These results indicate cryoablation triggers a Th2 biased response which can be shifted toward a Th1 response with addition of CpG. However, CpG treatment alone was unable to mediate tumor regression despite elevated Ab levels, which argues for concurrent tumor debulking.

To test if α-neu Ab mediates tumor rejection, we performed an adoptive serum transfer experiment. A single injection of serum from naïve mice, mice treated with cryoablation + CpG or pNeuE2 vaccination, or monoclonal Ab4, were injected into mice inoculated 3 days earlier with TUBO. Cryoablation + CpG serum greatly reduced TUBO growth relative to control serum (p<0.01), and had equivalent activity relative to pNeuE2 vaccination serum and monoclonal Ab4 (Supplementary Fig. S2). Therefore, α-neu Ab induced by cryoablation + CpG plays a significant role in controlling tumor growth.

Tumor specific cellular activity was assessed from tumor draining lymph node cells (TDLNs) and splenocytes after *in vitro* neu stimulation. IFN-γ ELISPOT and 10-plex cytokine analyses of mice treated with cryoablation or cryoablation + CpG showed minimal cytokine production relative to untreated tumor bearing controls (not shown) despite the significant changes in α-neu IgG. Together these results suggest negligible T-cell activation by cryoablation + CpG of TUBO.

Cryoablation and α-neu immunity in neu-tolerant BALB/NeuT and immunodeficient SCID mice

Cryoablation of neu[+] TUBO was further tested in BALB/NeuT mice, which express a transforming rat *neu* and exhibit immune tolerance to neu (30, 31). Initial studies found cryoablation, with or without CpG injection, insufficient to induce α-neu Ab, consistent with immune tolerance to neu (not shown). As in breast cancer patients, moderate α-neu immunity can be induced in NeuT mice by DNA vaccination (43, 44).Therefore, we tested if cryoablation impacts vaccine induced immunity in these mice. To establish α-neu immunity, NeuT males were inoculated with TUBO and subsequently electrovaccinated using pNeuE2 at 2 and 4 days after TUBO inoculation (Fig. 4A). When tumors were ~60mm^3 in size mice were treated with cryoablation ± CpG or excision. The majority of tumors treated with cryoablation alone recurred after initial regression, whereas only 1/8 mice treated with cryoablation + CpG developed local recurrence (Fig. 4B). Recurrences were compiled from 2 independent experiments using NeuT males treated with cryoablation alone, cryoablation + CpG, or excision. All mice were treated when tumors were ~60mm^3 and monitored for 40-60 days (Fig. 4C). Cryoablation alone had a recurrence rate of ~71%, with recurrences detected between 30-43 days after cryoablation. When CpG was combined with cryoablation the recurrence rate fell to 12%. No recurrences were detected with excision.

To simulate undetected systemic disease, mice received a secondary TUBO inoculation on the contralateral side 15 days after cryoablation. Neither cryoablation, with or without CpG, altered vaccine induced α-neu IgG (Fig. 4D) or protected mice from secondary tumor growth (Fig. 4E-F). Despite the lack of adaptive immune modulation, addition of CpG significantly reduced recurrences to a similar level as that of excision. To determine if this protective effect was mediated by innate immunity, recurrence rates of cryoablation alone and cryoablation + CpG were compared in TUBO bearing SCID mice (Fig. 4G). All mice were treated when tumors were ~60mm^3 and monitored for 65 days. Treatment with cryoablation + CpG significantly delayed tumor recurrence by >2 weeks, although all but one tumor eventually recurred, indicating partial protection by innate immunity and the importance of adaptive immunity for long-term protection.

Cryoablation of D2F2/E2 mammary adenocarcinoma

The impact of cryoablation was further tested in D2F2/E2 mammary adenocarcinoma which, unlike TUBO, induces significant levels of α-Her2 IgG1 and splenocyte IFN-γ response without exogenous intervention (Supplementary Fig. S3). However, this endogenous α-Her2 immunity is insufficient to prevent progressive tumor growth. Thus, D2F2/E2 may be representative of Her2^{+} tumors which are immunogenic but refractory to Her2 targeted therapy (34, 45). BALB/c mice were inoculated with D2F2/E2 cells and when tumors reached ~60mm^3 they were treated with cryoablation ± CpG, CpG injection alone, tumor excision, or sham surgery (Fig. 5A). All tumors treated with cryoablation ± CpG or surgical excision completely regressed by day 41 with the exception of one mouse in the cryoablation alone group that developed a recurrence on day 29. CpG treatment alone did not significantly change tumor growth relative to untreated mice (Fig. 5B).

Once cryoablated tumors had fully resolved (~7 wks), tumor-free mice received a secondary D2F2/E2 inoculation on the contralateral side to simulate outgrowth of a distant tumor. Treatment of the primary D2F2/E2 tumor with excision or cryoablation ± CpG resulted in similar protection from the secondary inoculation (~70-85%) (Fig. 5C), suggesting that α-Her2 immunity induced by D2F2/E2 tumor growth renders systemic protection once the primary tumor is ablated, regardless of the treatment modality. By day 59 mice treated with cryoablation ± CpG or tumor excision produced comparable levels of IFN-γ after *in vitro* Her2 stimulation of secondary TDLNs, which was significantly elevated relative to naïve mice, illustrating host reactivity to D2F2/E2 tumor growth (Fig. 5D). Similar to TUBO, AUC analysis of α-Her2 IgG1 found no significant difference between treatment groups, but IgG2a levels were significantly elevated when cryoablation and CpG were used concurrently, further supporting the notion of a Th1 shifted response. These results indicate that α-Her2 immunity is induced by D2F2/E2 tumor growth and exerts systemic protection after tumor resolution.

Similar to TUBO, primary D2F2/E2 tumors recurred after cryoablation in a fraction of mice, and these results were compiled from 4 independent experiments to include mice treated with either cryoablation alone or cryoablation + CpG. All mice were treated when tumors were ~60mm^3 and monitored for 30-60 days (Fig. 5F). Cryoablation alone had a recurrence rate of ~29%, with recurrences detected between 24-58 days. When combined with CpG the recurrence rate fell to 0%, consistent with activation of innate immunity and manifestation of endogenous adaptive immunity.

Transient immune refractory period after cryoablation

Although cryoablation of D2F2/E2 protected mice from a second inoculation once the ablated tumor had completely resolved, the presence of resolving necrotic tumor along with wound healing and inflammation may affect the growth of a co-existing tumor. Thus, we tested the level of tumor protection and growth during the wound healing phase. D2F2/E2 tumor-bearing mice were treated as previously described and a second inoculation was administered on day 13 during the wound healing phase (Fig. 6A). With cryoablation, 1/9 (12%) mice were protected from the second inoculation (Fig. 6B), compared to 4/5 (80%) mice when inoculated after tumor resolution (day 41) (Fig. 5C). Addition of CpG in combination with cryoablation resulted in improved protection with 8/16 (50%) mice rejecting the second inoculation, compared to 5/6 (80%) after tumor resolution. Secondary tumors that grew in cryoablation ± CpG treated mice grew at comparable rates to untreated mice, while tumors in the excision group grew significantly slower relative to cryoablation alone (Fig. 6C). All groups had significantly delayed secondary tumor growth relative to naïve mice, indicating partial tumor inhibition by endogenous α-Her2 immunity (Fig. 6C). As expected, all tumorexperienced mice produced elevated α-Her2 splenocyte IFN-γ responses relative to naïve mice, however there was no significant difference between treatment groups (Fig. 6D). Therefore, resolving necrotic tumor left by cryoablation results in a transient immune refractory period relative to tumor excision, which can partially be abrogated with CpG.

Peritumoral CpG treatment activates innate and adaptive immunity

Peritumoral CpG injection reduces cryoablation recurrences independent of adaptive immunity as observed with NeuT mice (Fig. 4). To evaluate systemic effects from CpG treatment, cytokine levels were examined in plasma on day 2 and 12 after treatment with 10-plex cytokine analyses (Fig. 7A). On day 2, plasma mice treated with CpG, either alone or in combination with cryoablation, showed significant increases in IL-1β, IL-6, IL-12, IFN-γ, and TNF-α relative to all other groups, indicating acute inflammation (Fig. 7B). By day 12 most cytokine levels had subsided, with the exception of IL-12 which remained significantly elevated after CpG treatment.

Local and systemic tumor specific immunity was assessed from TDLNs and splenocytes harvested on day 12 with *in vitro* Her2 stimulation. IFN-γ production from TDLNs with CpG treatment, with or without cryoablation, was significantly elevated, but no significant differences were found between treatment groups in splenocytes, suggesting CpG effects on adaptive immunity are regionalized to the injection site (Fig. 7C). There was a 3x increase in circulating DCs (CD11c^{+}) 2 days after CpG treatment with or without cryoablation (Fig. 7D). Natural killer (NK) cells (CD49b^{+}) also significantly increased after treatment with cryoablation + CpG. Similar to plasma cytokine levels, this increase in both DCs and NK cells was transient and dissipated by day 12 (not shown). Therefore, peritumoral CpG injection strongly activates innate immunity and enhances regional adaptive responses with D2F2/E2.

Discussion

We show that cryoablation of neu[+] TUBO in BALB/c mice resulted in systemic immune priming and tumor protection, but had little impact in neu-tolerant NeuT mice. Cryoablation of Her2^{+} D2F2/E2 enabled the functionality of tumor-induced immunity but secondary tumors were refractory if rechallenge occurred during the resolution phase of the cryoablated tumor. CpG following cryoablation significantly eliminated, reduced, or delayed tumor recurrences in WT, neu-tolerant, and SCID mice respectively. Therefore, tumor antigens released by cryoablation induce varying levels of innate and adaptive immunity in different host environments which is enhanced by CpG. Importantly, innate immunity induced by CpG plays a critical role in controlling local tumor recurrences.

Cryoablation of TUBO in WT mice resulted in α-neu IgG production and systemic protection in the majority of mice. In contrast to previous reports (4), resulting immunity was not Th1 biased but favored a Th2 response as evident by a dominant IgG1 Ab response, and little T-cell activation. To reverse Th2 biased immunity, the Th1 promoting TLR9 agonist CpG was tested in combination with cryoablation. Although CpG monotherapy of TUBO was not capable of mediating tumor regression, cryoablation + CpG resulted in a dramatic increase in α-neu IgG and shifted the response toward Th1, as evident by increased IgG2a levels. A similar, albeit less dramatic enhancement in IgG2a was also observed with D2F2/E2. This response protected nearly 100% of TUBO-bearing mice from secondary inoculation. These findings are further corroborated by Nierkens and den Brok, who reported similar enhanced protection with combined CpG treatment (10, 25).

Notably, tumor recurrences of both TUBO and D2F2/E2 dropped to 0% in WT mice and to 12% in NeuT mice when CpG was concurrently used. Innate immunity significantly contributes to this effect as evident by the delay in tumor recurrence seen in SCID mice. However, long-term recurrence-free survival is dependent on the capacity of adaptive immunity, which is shown by the step-wise increase in recurrences observed in WT, tolerant NeuT, and SCID mice. Increased levels of cytokines, including IFN-γ and IL-12, correlated with increased levels of circulating DCs and NK cells 2 days after CpG treatment, consistent with innate immunity activation (24, 42). Additionally, CpG may also promote the tumoricidal properties of infiltrating macrophages (23) following cryoablation (Fig. 1). For high-risk tumors and oligometastatic disease, residual tumor microfoci and subsequent recurrence is a significant clinical consideration following cryoablation (46, 47). The added protection provided by CpG may expand the utility of cryoablation to successfully treat more patients. Furthermore, local CpG injection may enable cryoablation to completely ablate lesions without requiring standard freeze margins, such as nerve sparing prostate cryoablation, which warrants further investigation.

Cryoablation of D2F2/E2 uncovered a transient immune refractory period lasting until the residual necrotic tumor resolved. To begin elucidating the mechanism we analyzed circulating populations of T-regulatory cells (Tregs), myeloid derived suppressor cells, as well as IL-10 and TGF-β production without finding any significant differences relative to excision or cryoablation + CpG treated mice (not shown). However, these findings do not exclude the possibility of another source of immunosuppression.

Despite finding significant increases in α-neu Ab after treatment of TUBO tumors we did not observe significant changes in tumor specific T-cell activity between treatment groups. Cryoablation may activate T-cells which are recruited to a compartment other than the spleen or TDLNs, such as the necrotic tumor. Alternatively, the frequency of α-neu T-cells may be lower than the detection limit of our assay system. We also tested if cryoablation generated a broader anti-tumor response by challenging cryoablated treated D2F2/E2 bearing mice with Her2 negative D2F2 tumor. No inhibition of tumor growth was observed reflecting a limited response to the dominant tumor antigen (not shown).

Our results, along with CpG clinical trial findings (18, 48), highly support concurrent CpG treatment with cryoablation to improve local tumor control with the potential to induce or amplify systemic tumor-specific immunity. Although not tested in this study, the use of therapeutics directly targeting immunosuppressive cells, such as Tregs (11, 49, 50), has enhanced cryoablation immune responses, and may further improve responses using cryoablation + CpG treatment, especially in tolerant hosts. Other means of redirecting tissue inflammation toward a Th1 response and promoting CD8 T-cell activation following cryoablation may also improve outcomes with cryoablation. As new immunotherapeutic options emerge, it is essential to understand the mechanisms by which cryoablation affects antitumor immunity so an appropriate combination of therapeutic interventions can be used to improve clinical outcomes.

Supplementary Material

Refer to Web version on PubMed Central for supplementary material.

Acknowledgments

References

1. Korpan NN. A history of cryosurgery: its development and future. J AmCollSurg. 2007; 204:314–24.

2. Hoffmann NE, Bischof JC. The cryobiology of cryosurgical injury. Urology. 2002; 60:40–9. [PubMed: 12206847]

3. Littrup PJ, Jallad B, Chandiwala-Mody P, D'Agostini M, Adam BA, Bouwman D. Cryotherapy for breast cancer: a feasibility study without excision. J VascIntervRadiol. 2009; 20:1329–41.

4. Sabel MS. Cryo-immunology: a review of the literature and proposed mechanisms for stimulatory versus suppressive immune responses. Cryobiology. 2009; 58:1–11. [PubMed: 19007768]

5. Soanes WA, Gonder MJ, Ablin RJ. A possible immuno-cryothermic response in prostatic cancer. ClinRadiol. 1970; 21:253–5.

6. Blackwood J, Moore FT, Pace WG. Cryotherapy for malignant tumors. Cryobiology. 1967; 4:33–8. [PubMed: 5582233]

7. Si T, Guo Z, Hao X. Immunologic response to primary cryoablation of high-risk prostate cancer. Cryobiology. 2008; 57:66–71. [PubMed: 18593573]

8. Thakur A, Littrup P, Paul EN, Adam B, Heilbrun LK, Lum LG. Induction of specific cellular and humoral responses against renal cell carcinoma after combination therapy with cryoablation and granulocyte-macrophage colony stimulating factor: a pilot study. J Immunother. 2011; 34:457–67. [PubMed: 21577139]

9. Sabel MS, Nehs MA, Su G, Lowler KP, Ferrara JL, Chang AE. Immunologic response to cryoablation of breast cancer. Breast Cancer Res Treat. 2005; 90:97–104. [PubMed: 15770533]

10. Nierkens S, den Brok MH, Sutmuller RP, Grauer OM, Bennink E, Morgan ME, et al. In vivo colocalization of antigen and CpG [corrected] within dendritic cells is associated with the efficacy of cancer immunotherapy. Cancer Res. 2008; 68:5390–6. [PubMed: 18593941]

11. den Brok MH, Sutmuller RP, Nierkens S, Bennink EJ, Frielink C, Toonen LW, et al. Efficient loading of dendritic cells following cryo and radiofrequency ablation in combination with immune modulation induces anti-tumour immunity. BrJCancer. 2006; 95:896–905.

12. Hoffmann NE, Coad JE, Huot CS, Swanlund DJ, Bischof JC. Investigation of the mechanism and the effect of cryoimmunology in the Copenhagen rat. Cryobiology. 2001; 42:59–68. [PubMed: 11336490]

13. Matsumura K, Sakata K, Saji S, Misao A, Kunieda T. Antitumor immunologic reactivity in the relatively early period after cryosurgery: experimental studies in the rat. Cryobiology. 1982; 19:263–72. [PubMed: 7105778]

14. Muller LC, Micksche M, Yamagata S, Kerschbaumer F. Therapeutic effect of cryosurgery of murine osteosarcoma--influence on disease outcome and immune function. Cryobiology. 1985; 22:77–85. [PubMed: 3856507]

15. Yamashita T, Hayakawa K, Hosokawa M, Kodama T, Inoue N, Tomita K, et al. Enhanced tumor metastases in rats following cryosurgery of primary tumor. Gann. 1982; 73:222–8.

16. Urano M, Tanaka C, Sugiyama Y, Miya K, Saji S. Antitumor effects of residual tumor after cryoablation: the combined effect of residual tumor and a protein-bound polysaccharide on multiple liver metastases in a murine model. Cryobiology. 2003; 46:238–45. [PubMed: 12818213]

17. Friedman EJ, Orth CR, Brewton KA, Ponniah S, Alexander RB. Cryosurgical ablation of the normal ventral prostate plus adjuvant does not protect Copenhagen rats from Dunning prostatic adenocarcinoma challenge. JUrol. 1997; 158:1585–8. [PubMed: 9302178]

18. Klinman DM. Immunotherapeutic uses of CpG oligodeoxynucleotides. Nature reviews Immunology. 2004; 4:249–58.

19. Klinman DM, Yi AK, Beaucage SL, Conover J, Krieg AM. CpG motifs present in bacteria DNA rapidly induce lymphocytes to secrete interleukin 6, interleukin 12, and interferon gamma. Proc Natl Acad Sci U S A. 1996; 93:2879–83. [PubMed: 8610135]

20. Sun S, Zhang X, Tough DF, Sprent J. Type 1 interferon-mediated stimulation of T cells by CpG DNA. JExpMed. 1998; 188:2335–42.

21. Ballas ZK, Rasmussen WL, Krieg AM. Induction of NK activity in murine and human cells by CpG motifs in oligodeoxynucleotides and bacterial DNA. J Immunol. 1996; 157:1840–5. [PubMed: 8757300]

22. Halpern MD, Kurlander RJ, Pisetsky DS. Bacterial DNA induces murine interferon-gamma production by stimulation of interleukin-12 and tumor necrosis factor-alpha. Cell Immunol. 1996; 167:72–8. [PubMed: 8548847]

23. Auf G, Carpentier AF, Chen L, Le Clanche C, Delattre JY. Implication of macrophages in tumor rejection induced by CpG-oligodeoxynucleotides without antigen. Clin Cancer Res. 2001; 7:3540–3. [PubMed: 11705874]

24. Kalinski P, Moser M. Consensual immunity: success-driven development of T-helper- 1 and T-helper-2 responses. Nature reviews Immunology. 2005; 5:251–60.

25. den Brok MH, Sutmuller RP, Nierkens S, Bennink EJ, Toonen LW, Figdor CG, et al. Synergy between in situ cryoablation and TLR9 stimulation results in a highly effective in vivo dendritic cell vaccine. Cancer Res. 2006; 66:7285–92. [PubMed: 16849578]

26. Nierkens S, den Brok MH, Roelofsen T, Wagenaars JA, Figdor CG, Ruers TJ, et al. Route of administration of the TLR9 agonist CpG critically determines the efficacy of cancer immunotherapy in mice. PloS one. 2009; 4:e8368. [PubMed: 20020049]

27. Dhar N, Ward JF, Cher ML, Jones JS. Primary full-gland prostate cryoablation in older men (> age of 75 years): results from 860 patients tracked with the COLD Registry. BJU international. 2011; 108:508–12. [PubMed: 21722288]

28. Guillotreau J, Haber GP, Autorino R, Miocinovic R, Hillyer S, Hernandez A, et al. Robotic partial nephrectomy versus laparoscopic cryoablation for the small renal mass. European urology. 2012; 61:899–904. [PubMed: 22264680]

29. Matsushima H, Ogawa Y, Miyazaki T, Tanaka H, Nishibu A, Takashima A. Intravital imaging of IL-1beta production in skin. The Journal of investigative dermatology. 2010; 130:1571–80. [PubMed: 20147964]

30. Lucchini F, Sacco MG, Hu N, Villa A, Brown J, Cesano L, et al. Early and multifocal tumors in breast, salivary, harderian and epididymal tissues developed in MMTY-Neu transgenic mice. Cancer Lett. 1992; 64:203–9. [PubMed: 1322235]

31. Boggio K, Nicoletti G, Di CE, Cavallo F, Landuzzi L, Melani C, et al. Interleukin 12-mediated prevention of spontaneous mammary adenocarcinomas in two lines of Her-2/neu transgenic mice. J ExpMed. 1998; 188:589–96.

32. Rovero S, Amici A, Carlo ED, Bei R, Nanni P, Quaglino E, et al. DNA vaccination against rat her-2/Neu p185 more effectively inhibits carcinogenesis than transplantable carcinomas in transgenic BALB/c mice. J Immunol. 2000; 165:5133–42. [PubMed: 11046045]

33. Mahoney KH, Miller BE, Heppner GH. FACS quantitation of leucine aminopeptidase and acid phosphatase on tumor-associated macrophages from metastatic and nonmetastatic mouse mammary tumors. J LeukocBiol. 1985; 38:573–85.

34. Whittington PJ, Piechocki MP, Heng HH, Jacob JB, Jones RF, Back JB, et al. DNA vaccination controls Her-2+ tumors that are refractory to targeted therapies. Cancer Res. 2008; 68:7502–11. [PubMed: 18794138]

35. Wei WZ, Shi WP, Galy A, Lichlyter D, Hernandez S, Groner B, et al. Protection against mammary tumor growth by vaccination with full-length, modified human ErbB-2 DNA. Int J Cancer. 1999; 81:748–54. [PubMed: 10328228]

36. Jacob J, Radkevich O, Forni G, Zielinski J, Shim D, Jones RF, et al. Activity of DNA vaccines encoding self or heterologous Her-2/neu in Her-2 or neu transgenic mice. Cellular Immunology. 2006; 240:96–106. [PubMed: 16930573]

37. Vollmer J, Weeratna R, Payette P, Jurk M, Schetter C, Laucht M, et al. Characterization of three CpG oligodeoxynucleotide classes with distinct immunostimulatory activities. Eur J Immunol. 2004; 34:251–62. [PubMed: 14971051]

38. Wei WZ, Jacob JB, Zielinski JF, Flynn JC, Shim KD, Alsharabi G, et al. Concurrent induction of antitumor immunity and autoimmune thyroiditis in CD4+ CD25+ regulatory T cell-depleted mice. Cancer Research. 2005; 65:8471–8. [PubMed: 16166327]

39. Machin, D.; Cheung, YB.; Parmar, MKB.; Parmar, MKB. Survival analysis : a practical approach. 2. Chichester, England ; Hoboken, NJ: Wiley; 2006.

40. Gurtner GC, Werner S, Barrandon Y, Longaker MT. Wound repair and regeneration. Nature. 2008; 453:314–21. [PubMed: 18480812]

41. Park JM, Terabe M, Sakai Y, Munasinghe J, Forni G, Morris JC, et al. Early role of CD4+ Th1 cells and antibodies in HER-2 adenovirus vaccine protection against autochthonous mammary carcinomas. J Immunol. 2005; 174:4228–36. [PubMed: 15778385]

42. Restifo NP, Dudley ME, Rosenberg SA. Adoptive immunotherapy for cancer: harnessing the T cell response. Nature reviews Immunology. 2012; 12:269–81.

43. Norell H, Poschke I, Charo J, Wei WZ, Erskine C, Piechocki MP, et al. Vaccination with a plasmid DNA encoding HER-2/neu together with low doses of GM-CSF and IL-2 in patients with metastatic breast carcinoma: a pilot clinical trial. Journal of translational medicine. 2010; 8:53. [PubMed: 20529245]

44. Jacob JB, Quaglino E, Radkevich-Brown O, Jones RF, Piechocki MP, Reyes JD, et al. Combining human and rat sequences in her-2 DNA vaccines blunts immune tolerance and drives antitumor immunity. Cancer Res. 2010; 70:119–28. [PubMed: 20048073]

45. Nahta R, Yu D, Hung MC, Hortobagyi GN, Esteva FJ. Mechanisms of disease: understanding resistance to HER2-targeted therapy in human breast cancer. Nature clinical practice Oncology. 2006; 3:269–80.

46. Bang HJ, Littrup PJ, Currier BP, Goodrich DJ, Aoun HD, Klein LC, et al. Percutaneous cryoablation of metastatic lesions from non-small-cell lung carcinoma: initial survival, local control, and cost observations. Journal of vascular and interventional radiology : JVIR. 2012; 23:761–9. [PubMed: 22626267]

47. Bang HJ, Littrup PJ, Goodrich DJ, Currier BP, Aoun HD, Heilbrun LK, et al. Percutaneous cryoablation of metastatic renal cell carcinoma for local tumor control: feasibility, outcomes, and estimated cost-effectiveness for palliation. Journal of vascular and interventional radiology : JVIR. 2012; 23:770–7. [PubMed: 22538119]

48. Brody JD, Ai WZ, Czerwinski DK, Torchia JA, Levy M, Advani RH, et al. In situ vaccination with a TLR9 agonist induces systemic lymphoma regression: a phase I/II study. J Clin Oncol. 2010; 28:4324–32. [PubMed: 20697067]

49. Levy MY, Sidana A, Chowdhury WH, Solomon SB, Drake CG, Rodriguez R, et al. Cyclophosphamide Unmasks an Antimetastatic Effect of Local Tumor Cryoablation. The Journal of Pharmacology and Experimental Therapeutics. 2009:596–601. [PubMed: 19407102]

50. Waitz R, Solomon SB, Petre EN, Trumble AE, Fasso M, Norton L, et al. Potent induction of tumor immunity by combining tumor cryoablation with anti-CTLA-4 therapy. Cancer Res. 2012; 72:430–9. [PubMed: 22108823]
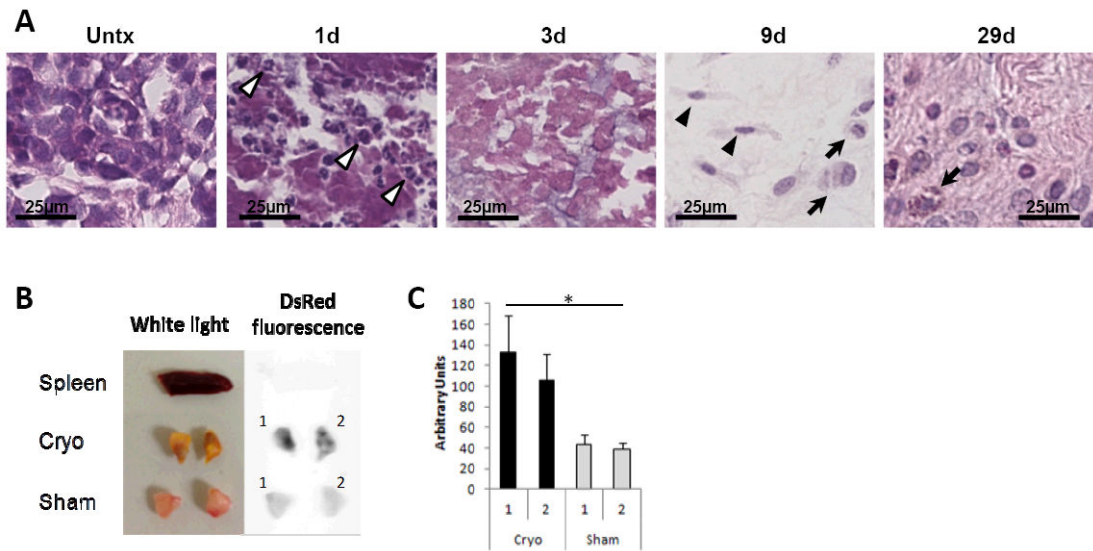
Figure 1. Necrosis and inflammatory infiltration following tumor cryoablation
(A) TUBO-bearing BALB/c mice were treated with cryoablation and tumors were harvested 1, 3, 9, and 29 days later (n=3-4). Representative H&E 100x images shown. Polymorphonucleocytes (white arrow heads), fibroblasts (black arrow heads), and macrophages (arrows). (B) D2F2/E2-bearing BALB/c pIL-1β-DsRed transgenic mice were treated with cryoablation or sham surgery (n=2). Tissues were harvested 15 days later for *ex vivo* imaging. Spleen was the control. (C) Mean DsRed fluorescence of each tumor slice was quantified using ImageJ densitometry software. *P<0.05 Unpaired ttest. Error bars, SD.
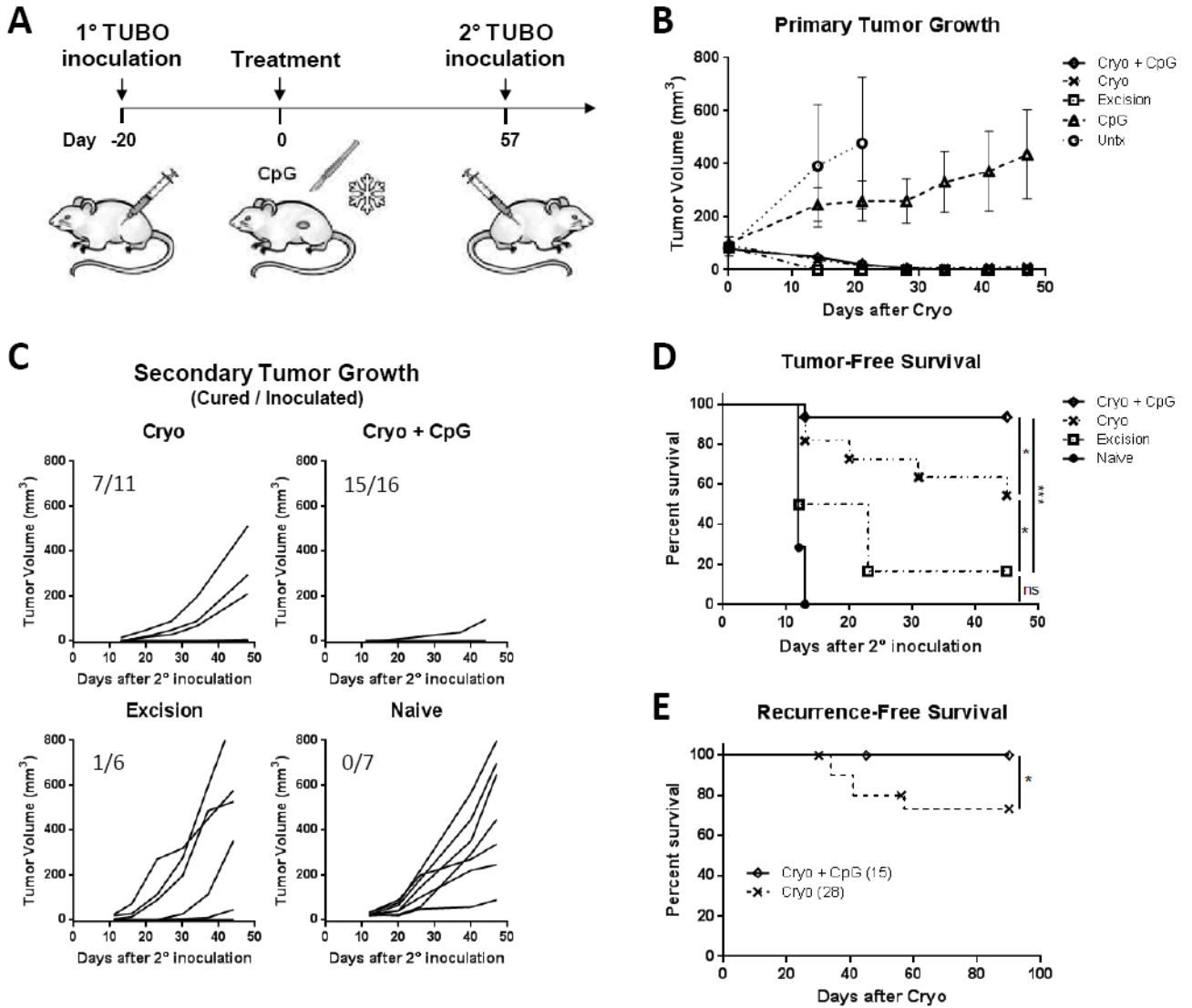
Figure 2. Cryoablation of TUBO tumor induces systemic antitumor protection and enhancement by CpG

(A) Experimental Scheme. (B) Primary TUBO growth. (C) Secondary tumor growth (cured/inoculated mice). (D) Tumor-free survival after secondary TUBO inoculation. Data pooled from 2 independent experiments. (E) Cryoablation recurrence data were pooled from 4 independent experiments. *$P<0.05$, ***$P<0.001$.
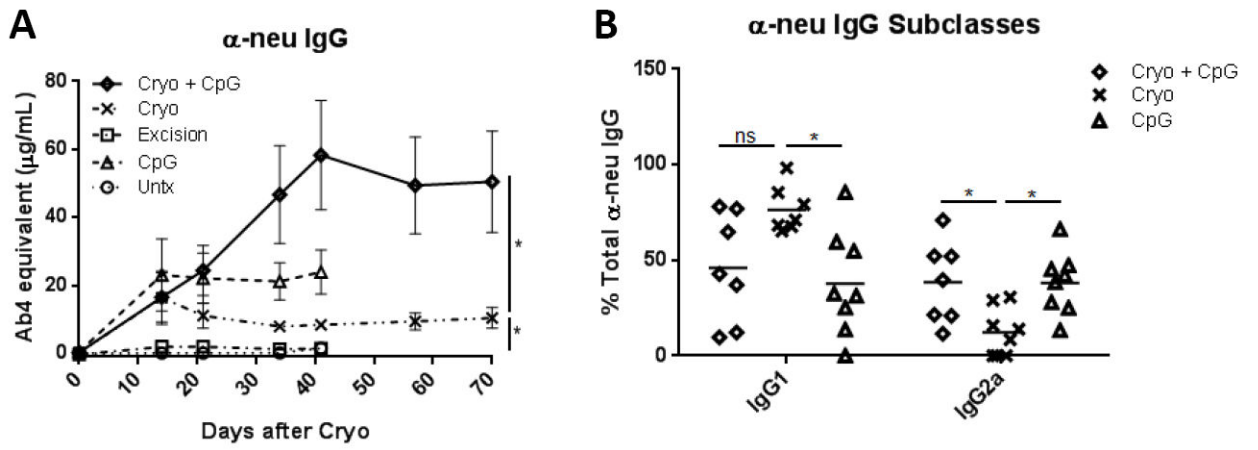
Figure 3. Cryoablation primarily induces α-neu IgG1 which is skewed toward IgG2a with the addition of CpG

Area under the curve analysis was performed for (A) total α-neu IgG. Unpaired t-test. (B) Percent total α-neu IgG was calculated for IgG2a and IgG1 subclasses. Data shown is representative of Ab subclass profile through day 70. *$P<0.05$.
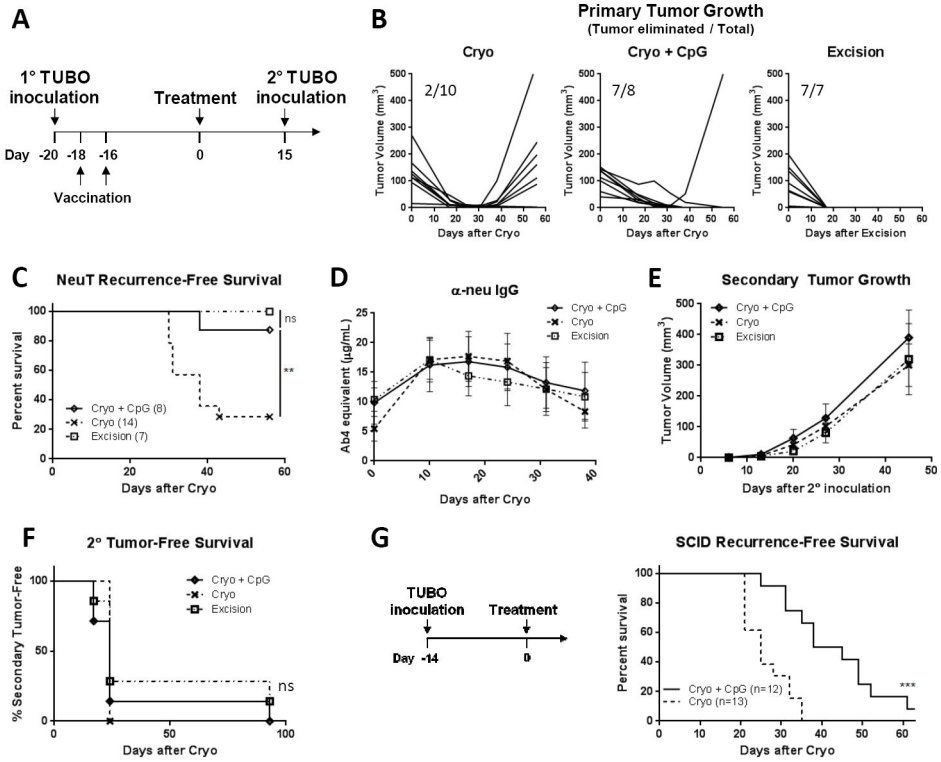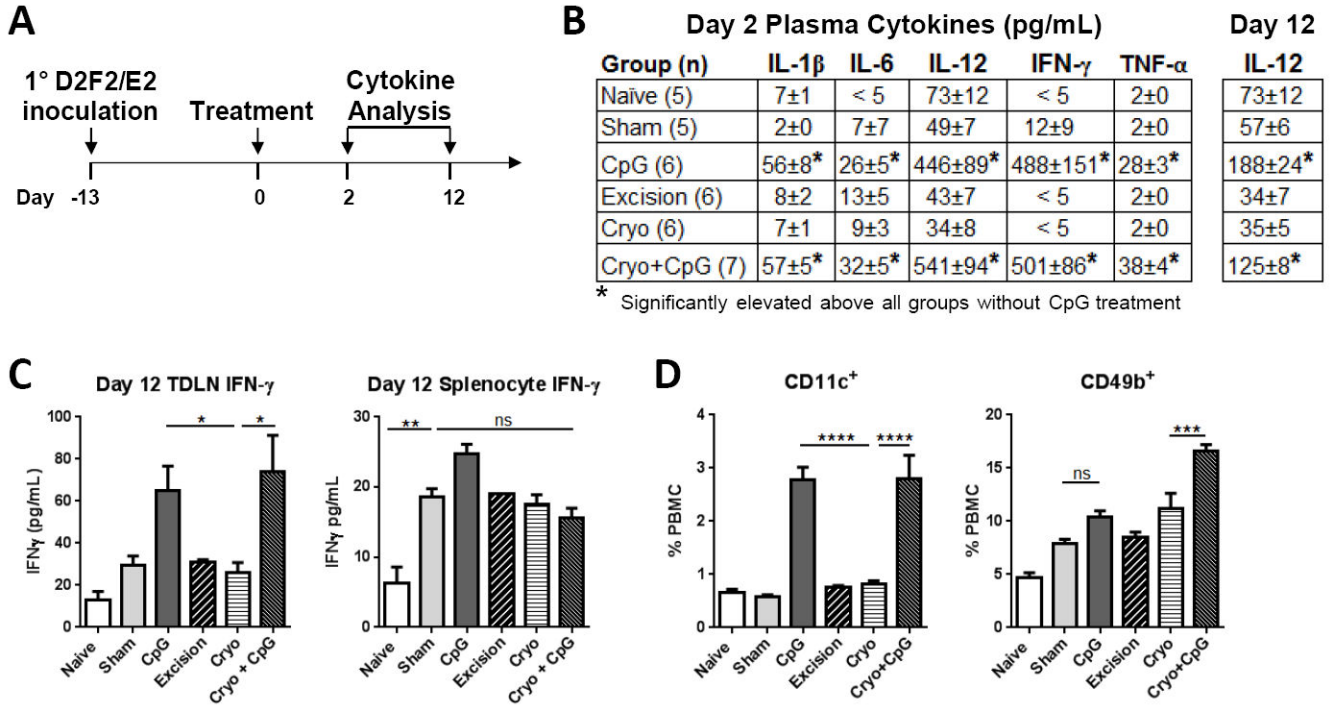
Figure 4. Cryoablation recurrences in tolerant NeuT and immunodeficient SCID mice are significantly reduced with CpG treatment

(A) Experimental scheme in male BALB/NeuT mice. (B) Primary TUBO tumor growth - (tumor eliminated/total). (C) NeuT recurrence-free survival - pooled from 2 independent experiments. (D) Total α-neu IgG. (E) Secondary tumor volume. (F) Protection from growth of secondary TUBO inoculation. (G) SCID experimental scheme and recurrence-free survival. **$P<0.01$, ***$P<0.001$.
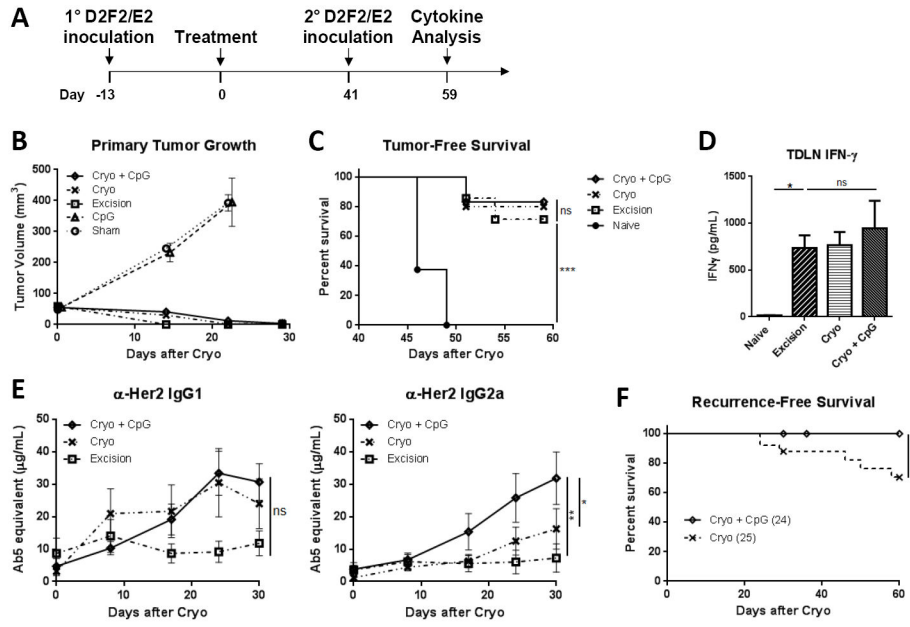
Figure 5. Complete resolution of D2F2/E2 tumor results in long-term protection
(A) Experimental scheme (n=6-7). (B) D2F2/E2 primary tumor growth. (C) Tumor-free survival after secondary D2F2/E2 inoculation. (D) Her2 stimulated TDLN IFN-γ production analyzed with Magpix. (E) α-Her2 IgG quantification. Area under the curve analysis was performed for α-neu IgG1 and IgG2a at day 30. (F) Cryoablation recurrence data were pooled from 4 independent experiments. *P<0.05, **P<0.01, ***P<0.001.
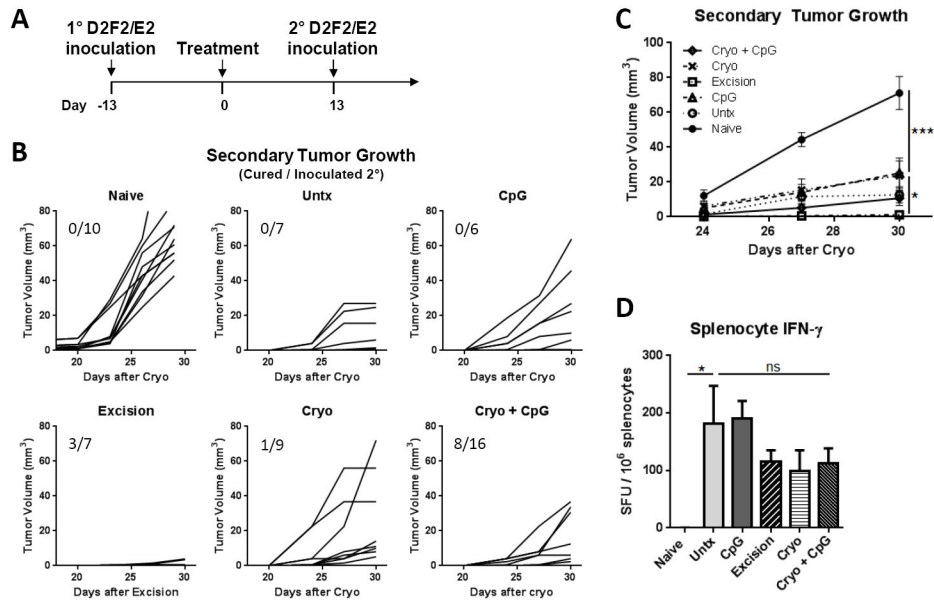
Figure 6. Cryoablation results in transient immune refractory period, which is partially abrogated with CpG

(A) Experimental scheme. (B) Secondary D2F2/E2 tumor growth – (cured/inoculated). (C) D2F2/E2 secondary tumor volume - pooled from 2 independent experiments. (D) Spleens were harvested 30 days after cryoablation for IFN-γ ELISPOT. *$P<0.05$, ***$P<0.001$.

A Experimental scheme.

B Day 2 Plasma Cytokines (pg/mL) / Day 12

Group (n)	IL-1β	IL-6	IL-12	IFN-γ	TNF-α	IL-12
Naïve (5)	7±1	< 5	73±12	< 5	2±0	73±12
Sham (5)	2±0	7±7	49±7	12±9	2±0	57±6
CpG (6)	56±8*	26±5*	446±89*	488±151*	28±3*	188±24*
Excision (6)	8±2	13±5	43±7	< 5	2±0	34±7
Cryo (6)	7±1	9±3	34±8	< 5	2±0	35±5
Cryo+CpG (7)	57±5*	32±5*	541±94*	501±86*	38±4*	125±8*

* Significantly elevated above all groups without CpG treatment

Figure 7. CpG treatment transiently increases inflammatory cytokines
(A) Experimental scheme. PBMC and plasma were collected 2 and 12 days after treatment. TDLNs and splenocytes were harvested on day 12 (2 independent experiments). (B) Plasma and (C) Her2 stimulated TDLN and splenocyte supernatants were analyzed with Magpix. (D) PBMCs were stained for TCRβ, CD11c, and CD49b for flow cytometry analysis (day 2). CD11c$^+$ and CD49b$^+$ populations initially gated on TCRβ$^-$ cells. *$P<0.05$, ***$P<0.001$ ****$P<0.0001$.